Enhanced second-harmonic generation from double resonant plasmonic antennae

Krishnan Thyagarajan,[1,2] Simon Rivier,[1,2] Andrea Lovera,[1] and Olivier J.F. Martin[1,*]

[1]*Nanophotonics and Metrology Laboratory (NAM), Swiss Federal Institute of Technology Lausanne (EPFL), 1015, Lausanne, Switzerland*
[2]*Both authors contributed equally to this work*
[*]*olivier.martin@epfl.ch*
www.nanophotonics.ch

Abstract: We present a novel plasmonic antenna geometry – the double resonant antenna (DRA) – that is optimized for second-harmonic generation (SHG). This antenna is based on two gaps coupled to each other so that a resonance at the fundamental and at the doubled frequency is obtained. Furthermore, the proximity of the localized hot spots allows for a coupling and spatial overlap between the two field enhancements at both frequencies. Using such a structure, both the generation of the second-harmonic and its re-emission into the far-field are significantly increased when compared with a standard plasmonic dipole antenna. Such DRA are fabricated in aluminium using electron beam lithography and their linear and nonlinear responses are studied experimentally and theoretically.

©2012 Optical Society of America

OCIS codes: (160.1245) Artificially engineered materials; (190.2620) Harmonic generation and mixing; (190.4350) Nonlinear optics at surfaces; (240.3695) Linear and nonlinear light scattering from surfaces; (240.6680) Surface plasmons; (250.5403) Plasmonics.

References and links

1. S. A. Maier, *Plasmonics: Fundamentals and Applications* (Springer, 2007).
2. E. Altewischer, M. P. van Exter, and J. P. Woerdman, "Plasmon-assisted transmission of entangled photons," Nature **418**(6895), 304–306 (2002).
3. T. Hanke, J. Cesar, V. Knittel, A. Trügler, U. Hohenester, A. Leitenstorfer, and R. Bratschitsch, "Tailoring spatiotemporal light confinement in single plasmonic nanoantennas," Nano Lett. **12**(2), 992–996 (2012).
4. D. Staedler, T. Magouroux, R. Hadji, C. Joulaud, J. Extermann, S. Schwung, S. Passemard, C. Kasparian, G. Clarke, M. Gerrmann, R. Le Dantec, Y. Mugnier, D. Rytz, D. Ciepielewski, C. Galez, S. Gerber-Lemaire, L. Juillerat-Jeanneret, L. Bonacina, and J.-P. Wolf, "Harmonic nanocrystals for biolabeling: a survey of optical properties and biocompatibility," ACS Nano **6**(3), 2542–2549 (2012).
5. S. Roke and G. Gonella, "Nonlinear light scattering and spectroscopy of particles and droplets in liquids," Annu. Rev. Phys. Chem. **63**(1), 353–378 (2012).
6. P. Mühlschlegel, H.-J. Eisler, O. J. F. Martin, B. Hecht, and D. W. Pohl, "Resonant optical antennas," Science **308**(5728), 1607–1609 (2005).
7. S. Palomba, M. Danckwerts, and L. Novotny, "Nonlinear plasmonics with gold nanoparticle antennas," J. Opt. A **11**(11), 114030 (2009).
8. T. Hanke, G. Krauss, D. Träutlein, B. Wild, R. Bratschitsch, and A. Leitenstorfer, "Efficient nonlinear light emission of single gold optical antennas driven by few-cycle near-infrared pulses," Phys. Rev. Lett. **103**(25), 257404 (2009).
9. A. Benedetti, M. Centini, C. Sibilia, and M. Bertolotti, "Engineering the second harmonic generation pattern from coupled gold nanowires," J. Opt. Soc. Am. B **27**(3), 408–416 (2010).
10. S. Lettieri, F. Gesuele, P. Maddalena, M. Liscidini, L. C. Andreani, C. Ricciardi, V. Ballarini, and F. Giorgis, "Second-harmonic generation in hydrogenated amorphous-SiN doubly resonant microcavities with periodic dielectric mirrors," Appl. Phys. Lett. **87**(19), 191110 (2005).
11. J. S. Levy, M. A. Foster, A. L. Gaeta, and M. Lipson, "Harmonic generation in silicon nitride ring resonators," Opt. Express **19**(12), 11415–11421 (2011).
12. F. Gesuele, S. Lettieri, P. Maddalena, M. Liscidini, L. C. Andreani, C. Ricciardi, V. Ballarini, and F. Giorgis, "Band-edge and cavity second harmonic conversion in doubly resonant microcavity," J. Phys. B **40**(4), 727–734 (2007).

13. H. Fischer and O. J. F. Martin, "Engineering the optical response of plasmonic nanoantennas," Opt. Express **16**(12), 9144–9154 (2008).
14. P. R. West, S. Ishii, G. V. Naik, N. K. Emani, V. M. Shalaev, and A. Boltasseva, "Searching for better plasmonic materials," Laser Photon. Rev. **4**(6), 795–808 (2010).
15. M. Castro-Lopez, D. Brinks, R. Sapienza, and N. F. van Hulst, "Aluminum for nonlinear plasmonics: resonance-driven polarized luminescence of Al, Ag, and Au nanoantennas," Nano Lett. **11**(11), 4674–4678 (2011).
16. M. Paulus and O. J. F. Martin, "Light propagation and scattering in stratified media: a Green's tensor approach," J. Opt. Soc. Am. A **18**(4), 854–861 (2001).
17. A. M. Kern and O. J. F. Martin, "Surface integral formulation for 3D simulations of plasmonic and high permittivity nanostructures," J. Opt. Soc. Am. A **26**(4), 732–740 (2009).
18. W. Zhang, B. Gallinet, and O. J. F. Martin, "Symmetry and selection rules for localized surface plasmon resonances in nanostructures," Phys. Rev. B **81**(23), 233407 (2010).
19. T. Xu, X. Jiao, G. P. Zhang, and S. Blair, "Second-harmonic emission from sub-wavelength apertures: effects of aperture symmetry and lattice arrangement," Opt. Express **15**(21), 13894–13906 (2007).
20. K. D. Ko, A. Kumar, K. H. Fung, R. Ambekar, G. L. Liu, N. X. Fang, and K. C. Toussaint, Jr., "Nonlinear optical response from arrays of Au bowtie nanoantennas," Nano Lett. **11**(1), 61–65 (2011).
21. S. Kujala, B. K. Canfield, M. Kauranen, Y. Svirko, and J. Turunen, "Multipolar analysis of second-harmonic radiation from gold nanoparticles," Opt. Express **16**(22), 17196–17208 (2008).
22. B. K. Canfield, H. Husu, J. Laukkanen, B. Bai, M. Kuittinen, J. Turunen, and M. Kauranen, "Local field asymmetry drives second-harmonic generation in non-centrosymmetric nanodimers," Nano Lett. **7**(5), 1251–1255 (2007).
23. B. K. Canfield, S. Kujala, K. Jefimovs, J. Turunen, and M. Kauranen, "Linear and nonlinear optical responses influenced by broken symmetry in an array of gold nanoparticles," Opt. Express **12**(22), 5418–5423 (2004).
24. B. K. Canfield, S. Kujala, K. Jefimovs, Y. Svirko, J. Turunen, and M. Kauranen, "A macroscopic formalism to describe the second-order nonlinear optical response of nanostructures," J. Opt. A, Pure Appl. Opt. **8**(4), S278–S284 (2006).
25. H. Husu, R. Siikanen, J. Mäkitalo, J. Lehtolahti, J. Laukkanen, M. Kuittinen, and M. Kauranen, "Metamaterials with tailored nonlinear optical response," Nano Lett. **12**(2), 673–677 (2012).
26. M. Gentile, M. Hentschel, R. Taubert, H. Guo, H. Giessen, and M. Fiebig, "Investigation of the nonlinear optical properties of metamaterials by second harmonic generation," Appl. Phys. B **105**(1), 149–162 (2011).

1. Introduction

The study of the nonlinear optical response of matter is important for various disciplines such as biology, information sciences and physics, especially when dealing with nanometer length scales [1–4]. It is therefore important to have efficient sources of nonlinear optical signals at such length scales. Second harmonic generation (SHG) is one such important nonlinear optical effect, which has the added advantage of being sensitive to symmetry. Under the dipole approximation, SHG is forbidden for centrosymmetric media; however since inversion symmetry is broken at an interface, one can use nonlinear SHG microscopy to study even centrosymmetric structures on surfaces [5]. It is well-known that plasmonic dipole antennae (DA) exhibit so-called hot spots in their gap, where the incident intensity can be enhanced by several orders of magnitude [6]. In recent years, experimental work [7, 8] and simulations [9] dealing with the SHG in dipole antennae have been reported. As the intensity of the second-harmonic signal is proportional to the square of the fundamental field intensity, this second-order nonlinear process can strongly benefit from the high enhancement of the incident field in these structures. Yet, all the previous studies in plasmonics rely on the enhancement of the fundamental field only and do not consider any resonance at the doubled frequency. This approach based on two resonances has been successfully demonstrated in traditional optics, for example in resonant Fabry-Perot microcavities [10–12]. In this work, we propose and experimentally demonstrate a novel plasmonic antenna geometry with two gaps that are coupled to each other, both of which exhibit a resonance at the fundamental and doubled frequency, and thus enhance simultaneously both the generation of the second-harmonic and its re-emission into the far-field.

2. Theoretical background and simulations

It is well known that the resonance of a dipole antenna can be spectrally tuned by varying the length of the antenna arms [13]. In the present work, the double resonant antenna (DRA) is

optimized for second-harmonic generation experiments using a Ti:sapphire laser centered at λ = 800 nm as pump source. The standard plasmonic materials for the visible region of the spectrum, gold and silver, are discarded for our study as they exhibit high losses due to interband transitions in the spectral region of the second-harmonic, which is at around λ = 400 nm [14]. On the contrary, aluminium shows intense localized surface plasmon resonances in the blue and UV region and is therefore more suited to study the effect of this second resonance on the SHG process, but shows interband transitions at the fundamental wavelength of 800 nm [14, 15].

The Green's tensor method is used to calculate and optimize the optical response of the DRA [16, 17], taking into account the influence of the substrate. The DRA consists of three rectangular arms with lengths of 50, 50 and 170 nm separated by a gap of 20 nm and width and height of 40nm as shown in the inset of Fig. 1(a). The intensity enhancement is calculated in the center of the two gaps of the DRA and, as seen in Fig. 1(a), is obtained in both gaps for the fundamental and the second-harmonic wavelengths. The proximity of the two gaps allows for a coupling of their resonances which is an important feature that sets this structure apart from other previous structures. An enhancement of roughly 30(20) at λ = 400nm and 35(180) at λ = 800 nm is found in the left (right) gap. It must be mentioned, that due to interband transitions near the fundamental wavelength, aluminium exhibits a slight damping of the resonance around λ = 800 nm [14]. Simulations show that the resonance at the second harmonic is mediated by a dipole appearing in the two short arms of the antenna, while the resonance at the fundamental frequency is controlled by the long arm of the aluminum antenna, as can be seen in Figs. 2(a) and 2(b). In plasmonic systems, additional resonances at short wavelength generally rely on multipolar resonances so that the re-emission of the signal to the far-field is limited [18]. With the unique geometry of this antenna, the second-harmonic signal can be optimally radiated into the far-field as a consequence of the strong radiating dipole. In addition, for the standard reference plasmonic DA resonant at the fundamental, simulations show that the field enhancement in the gap at the fundamental is higher than in the case of the DRA as can be seen in Fig. 1(b). The inset in Fig. 1(b) is a schematic of such a dipole antenna and Fig. 2(c) shows the local-field enhancement for the DA.
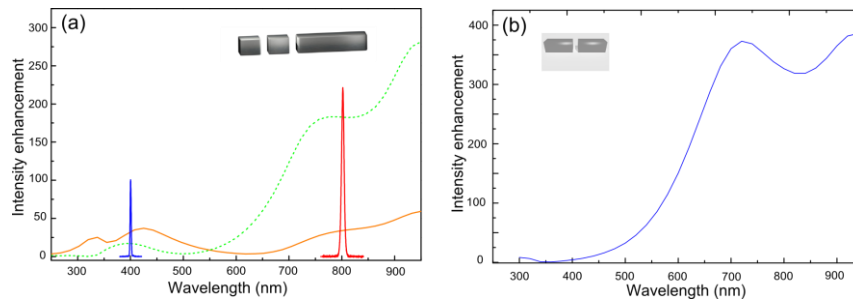

Fig. 1. (a) Intensity enhancement calculated in the center of both gaps (left gap: solid orange line, right gap: dashed green line) for the optimized DRA (50x50x170 nm^3). The blue and red peaks indicate spectra for the fundamental and SHG; (b) intensity enhancement at the gap in the dipole antenna. The insets show the geometries used.
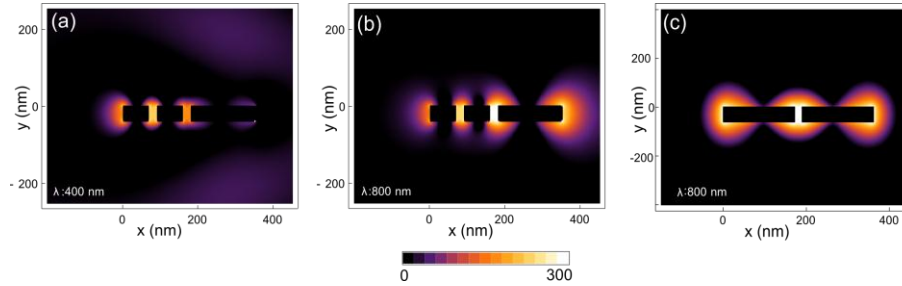
Fig. 2. Computed near-field intensity maps for (a) the resonance at λ = 400 nm, which is mediated by a radiating dipole in the two short arms, (b) the resonance at the fundamental at λ = 800 nm that is controlled by the long arm of the antenna, (c) the resonance at λ = 800 nm for the reference dipole antenna.

3. Experiments, results and discussion

The DRA and DA are prepared on a fused silica substrate using electron beam lithography with PMMA/MMA as bilayer resists. It should be noted that aluminium is prone to oxidation which can deteriorate the DRA quality; using the bilayer resists gives a decent undercut to define the DRA geometry. Arrays of 2500 antennae each are fabricated and the far-field SHG measurements shown in the paper correspond to the response of one such array. The fabricated gap sizes with a nominal dimension of 20 nm vary between 15 nm and about 25 nm over the entire array. The experimental setup used to characterize the fabricated structures is similar to ones that have been used earlier consisting of the laser and a lock-in detection [19]. For the SHG, a Ti:sapphire laser with 100 mW average output power and 150 fs average pulse duration is focused on the sample down to a spot diameter of approximately 25 μm using a 50 mm focal length achromat. The signal is collected with a microscope objective (Olympus 20x, 0.35 NA) and its power measured using a photomultiplier tube (Hamamatsu H 5784-20) with the help of a lock-in detection setup to obtain a good signal-to-noise ratio. Linear scattering spectra are measured with an Olympus IX71 dark field microscope (Olympus 60x, 0.7 NA) and a Jobin Yvon spectrometer (Triax 550). As can be seen in Fig. 3(a), the scattering is strongly enhanced for the DRA when compared to the standard plasmonic dipole antenna (DA) around λ = 400nm and λ = 800 nm, thanks to the double resonance. The standard plasmonic dipole antenna referred to here has dimensions of 170 nm x 40 nm x 40 nm and a gap of 20 nm; it has been designed to be resonant at the fundamental frequency. This leads to an enhanced SHG in the far-field as seen in Fig. 3(b): the DRA produces a SH intensity almost twice that of the DA.
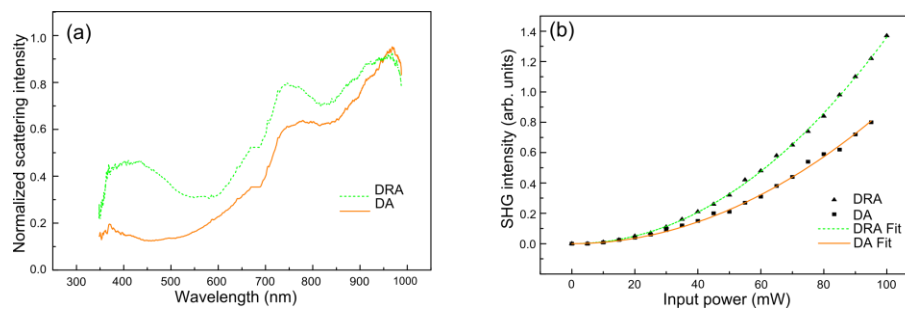

Fig. 3. (a) Scattering spectra of the standard dipole antenna (DA) and the double resonant antenna (DRA). The double structure shows a clear enhancement of the scattering around λ = 400nm, both structures are made of aluminium; (b) a comparison of the experimental SHG signal with a quadratic fit, for a DA and a DRA shows the enhanced SHG from the DRA.

The origin of this second harmonic signal is definitely in the DRA structures, where the plasmonic enhancement occurs. A spectrum showing the fundamental signal along with the signal at the second-harmonic is shown in Fig. 4(a). The second-harmonic signal is absent when the bare substrate is analyzed. Measurements such as that shown in Fig. 4(a) show negligible incoherent two-photon photoluminescence (TPPL) because they are taken at relatively low input powers. When the input power increases, the two-photon photoluminescence also increases as can be seen in the inset of Fig. 4(a), which shows increasing TPPL as pump powers are increased from 90mW up to 200mW. Polarization studies also show that the SHG signal is horizontally polarized (as shown in Fig. 4(b)), along the length of the DRA, which further indicates that the SHG originates from the DRA structures. One can see that the ratio of the SHG signal for the horizontal to the vertical polarization of the analyzer is about 10. The horizontal polarization can be fitted with a cosine squared function, showing that – as expected – only the horizontal input is resonant in these structures and furthermore there is a quadratic enhancement for the SHG.
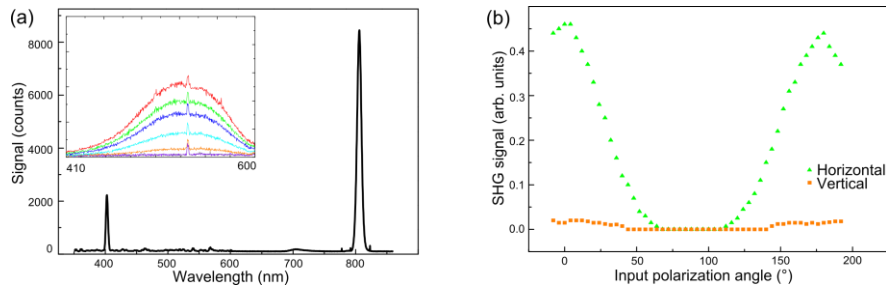

Fig. 4. (a) A spectrum showing the fundamental and the SHG for the DRA with an inset showing the two photon photoluminescence (TPPL), that was removed with filters for SHG measurements for different input powers – from 90mW up to 200mW, with counts of less than 1000; (b) polarization measurements of the SHG using horizontal (along antenna axis) and vertical detection for a DRA: the SHG is clearly polarized along the antenna.

Plasmonic dipole antennae have been studied earlier for SHG [20 and references therein] and have shown significant SHG due to the plasmonic enhancement of the fundamental field. SHG from such centrosymmetric structures has been attributed to the breaking of inversion symmetry at the surface. Furthermore, even slight deformations of the nanostructures can render the structures non-centrosymmetric, thereby allowing for SHG. At first glance, one would expect cancellation between the SHG sources from the two sides of the gap, but surface imperfections are sufficient to prevent this complete cancellation, thereby providing SHG in the far-field.

Despite this greater enhancement of the fundamental in the DA compared to DRA, the SHG in the far-field is larger with the DRA than the DA. This emphasizes that intensity enhancement of the fundamental is not the only sufficient criterion for enhanced SHG in the far-field.

4. Conclusions

We have proposed a double resonant plasmonic antenna with resonances both at the fundamental and second harmonic, such that a dipolar mode excited at the SH is radiated into the far field very effectively. Thanks to the coupling between the dipolar resonances in both arms at the two wavelengths, a noticeable SHG enhancement is observed, compared to a dipole antenna with a single resonance. This represents an improvement over structures that rely on higher order multipoles being excited at the second harmonic, since multipolar resonances inherently radiate less than a dipole. Another attractive feature of the DRA is that both dipolar resonances at both frequencies are spatially coupled. It is well known that the central symmetry of the nanostructures strongly influences the amount of second-harmonic

signal that is generated [21–26]. Indeed, in a structure with perfect symmetry, the electric dipole contribution vanishes and only the much weaker magnetic dipole and electric quadrupole remains. The SHG obtained from this novel DRA is a factor of two stronger than that for the DA. This modest improvement can be attributed to the fabrication difficulties associated with aluminium. We are currently improving the fabrication process and hope in the future to further improve the SHG enhancement from such structures.

Acknowledgments